ELECTRONIC SUPPLEMENTARY INFORMATION FILE of the paper published on PCCP

STRUCTURAL CHARACTERIZATION, THERMAL STABILITY AND PHARMACOKINETIC PROPERTIES OF ACTIVE MOLECULE/HYDROTALCITE (LDH) NANOCOMPOSITES

BY

ELEONORA CONTEROSITO, GIANLUCA CROCE, LUCA PALIN, CINZIA PAGANO, LUANA PERIOLI, DAVIDE VITERBO, ENRICO BOCCALERI, GEO PAUL, MARCO MILANESIO

ADDRESS: Dipartimento di Scienze e Innovazione Tecnologica and Nano-SiSTeMI Interdisciplinary Centre, Università del Piemonte Orientale "A. Avogadro" (Italy), Via Michel 11, I-15121 Alessandria, Italy.
Email: marco.milanesio@mfn.unipmn.it

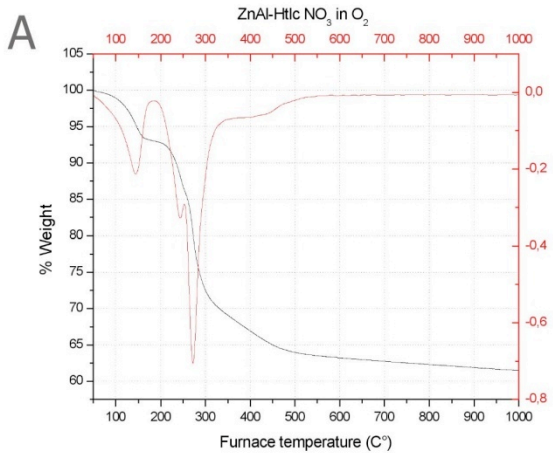
A
ZnAl-Htlc NO_3 in O_2
% Weight
Furnace temperature (C°)

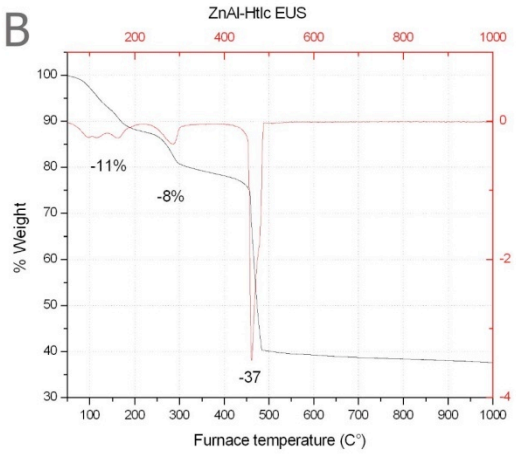
B
ZnAl-Htlc EUS
-11%
-8%
-37
% Weight
Furnace temperature (C°)

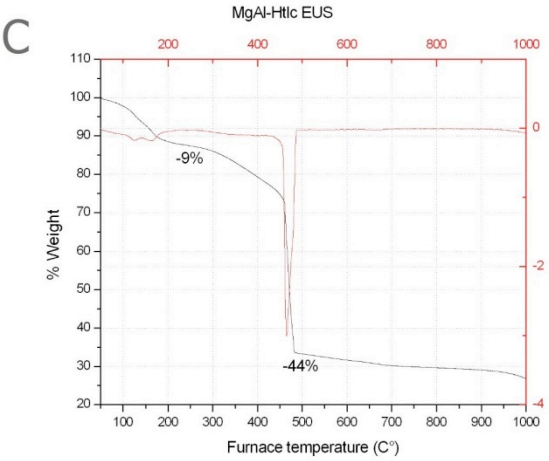
C
MgAl-Htlc EUS
-9%
-44%
% Weight
Furnace temperature (C°)

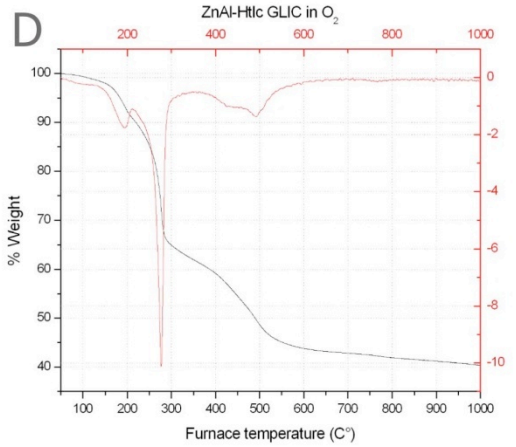
D
ZnAl-Htlc GLIC in O_2
% Weight
Furnace temperature (C°)

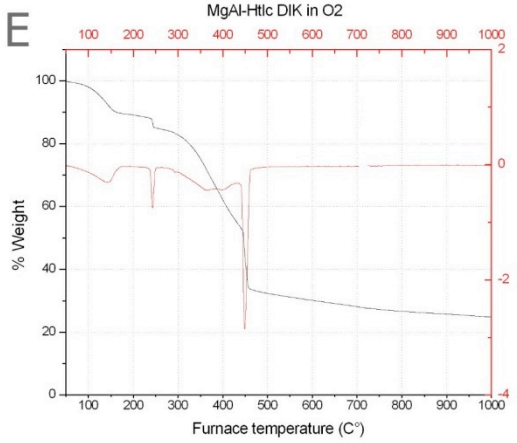
E
MgAl-Htlc DIK in O2
% Weight
Furnace temperature (C°)

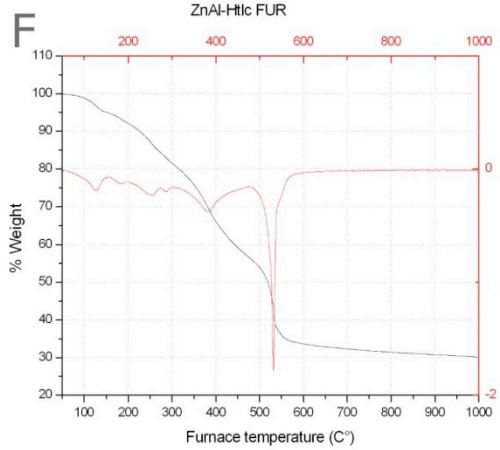
F
ZnAl-Htlc FUR
% Weight
Furnace temperature (C°)

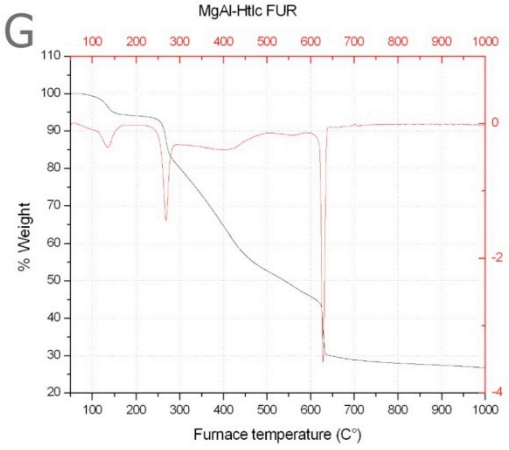
G
MgAl-Htlc FUR
% Weight
Furnace temperature (C°)

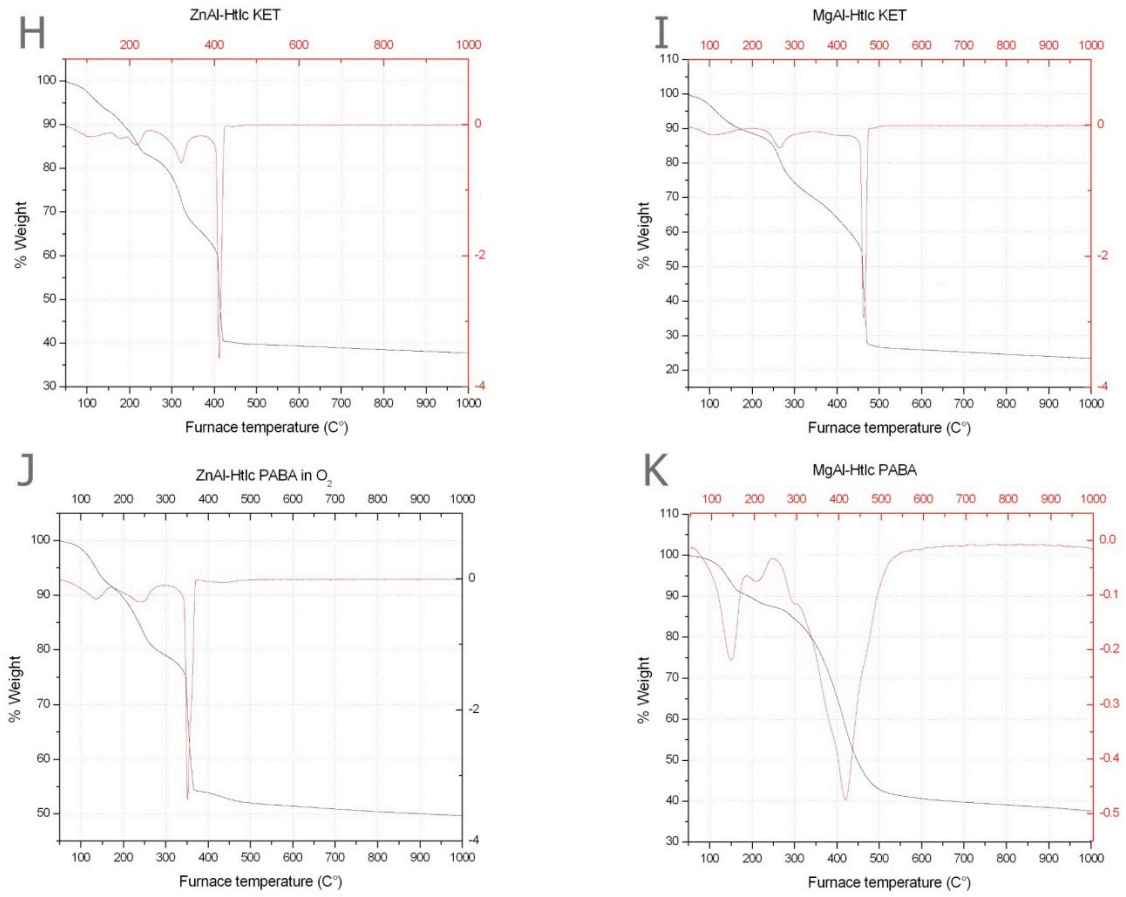

Figure SI1: TGA analyses (a) and derivative (b), carried out using 20ml/min O_2 flux and a temperature ramp of 10°C/min for nitrate (A), EUS (B and C), GLIC (D), DIK (E), KET (F and G), FURO (H and I) PABA (J and K) hydrotalcites.

The TGA curve of Zn/Al_LDH_NO_3 shows a loss of weight in the region between 70° and 200°C. The first weight loss (about 6-7%) is due to fisisorbed water while the second and more consistent (about 20%) weight loss between 200° and 300° C is due to the layer deoxydrilation. The last weight loss of the 5%, around 450°C, is finally attributable to the nitrate and the eventual carbonate.

TGA analysis was performed on all the samples and is reported for completeness although the same analysis on similar samples has been already published for the EUS[1], KET,[2] GLIC,[3] and DIK,[4] FURO[5] and PABA[6] samples. It is worth noting the difference between the curve of the Zn/Al sample and the Mg/Al one in almost all the cases, probably this is due to the different drug loading, already discussed in the paper and probably also to the different layer flexibility. In the Mg/Al_LDH_DIK and Mg/Al_LDH_FURO samples (Fig. SI1 E and G) the sharp peak of the derivative curve at about 250°C can be attributed to the loss of the organic compound that is adsorbed on the surfaces and not intercalated. The intercalate compound is loss at a higher temperature demonstrating the “shielding effect” of the intercalation.

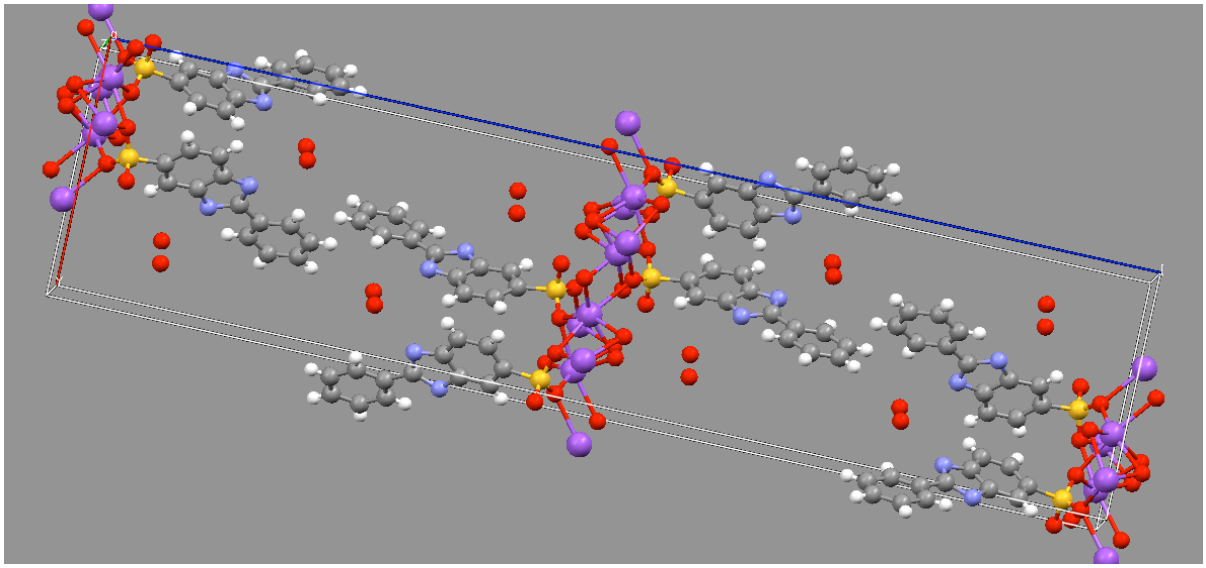

Figure SI2: Crystal packing of EUS_Na - The cell contains eight EUS molecules and four water molecules for each EUS unit. The sodium ion exhibits a distorted octahedral coordination environment with all the positions occupied by O-atoms, four belonging to the EUS molecule and two to water molecules. In the structure of the salt the proton is shared with adjacent water molecules and can be alternatively located either on one or the other N-atom. Layered-like structure is highlighted by the sodium disposition, used to calculate the stacking distance reported in table 4 in the manuscript. Color legend: sodium, purple; oxygen, red, carbon, grey, sulphur, yellow; nitrogen, light blue; hydrogen, white).

.

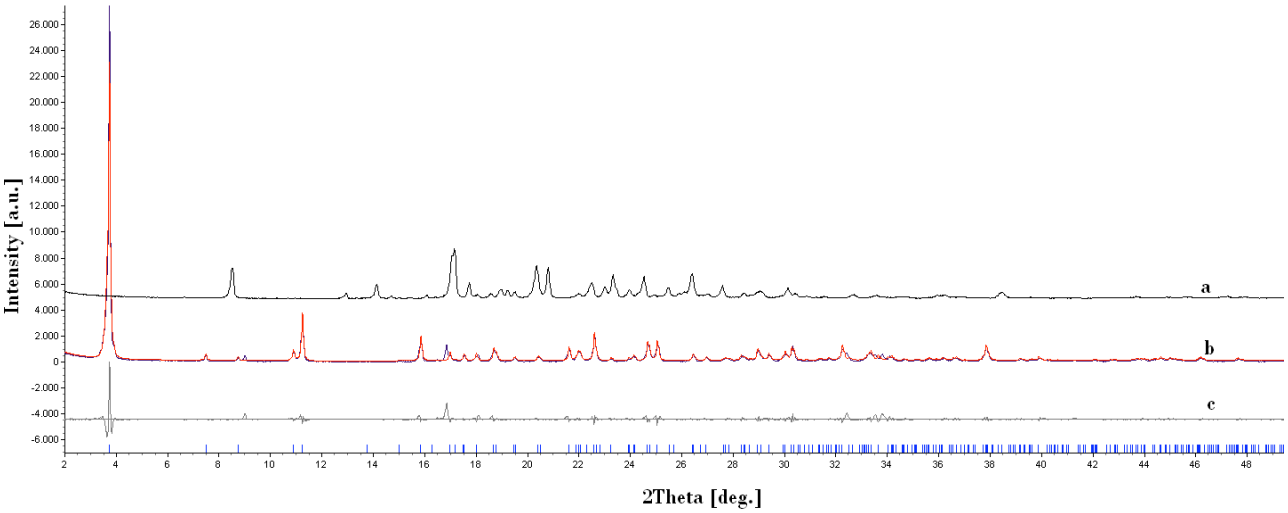

Figure SI3: Rietveld refinement (using the structure from single crystal data as reported in table SI1) of XRPD data from EUS_Na, proving that the sample used for SS-NMR and Raman spectroscopy analyses is homogeneous, approximately 95% pure (in fact only a very small un-indexed peak is present at $2\theta \approx 17°$) and statistically identical to the single crystal used to solve its structure. XRPD patterns of: (a) EUS acid to exclude its presence in experimental data and of (b) EUS_Na with in blue the experimental data and in red the calculated pattern. (c) is the difference curve between the observed and calculated pattern confirming the goodness of the fit.

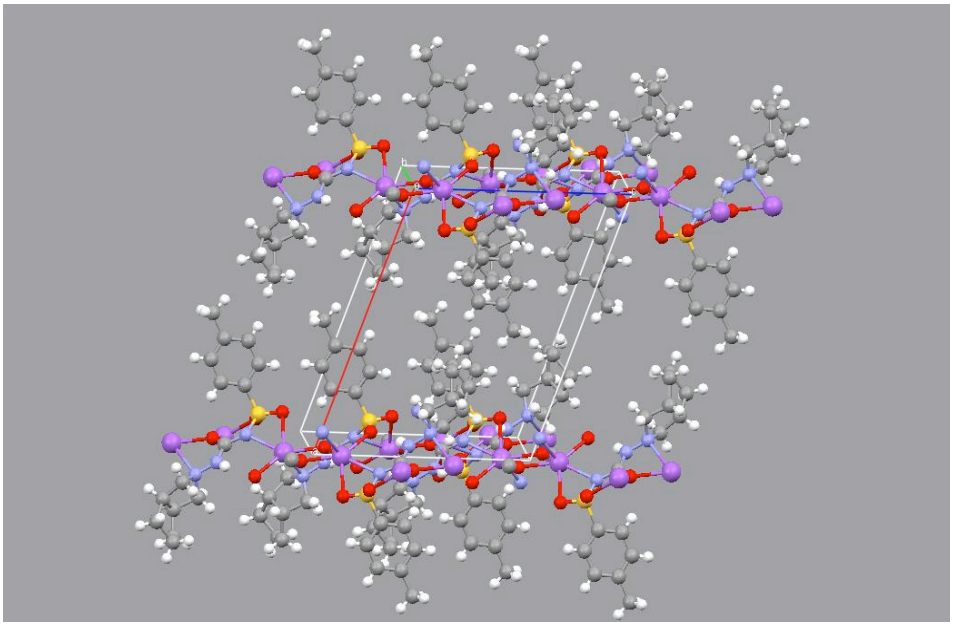

Figure SI4: Crystal packing of GLIC_Na. Layered-like structure is highlighted by the sodium (purple) disposition, used to calculate the stacking distance reported in table 4 in the manuscript; color legend as in figure SI2.

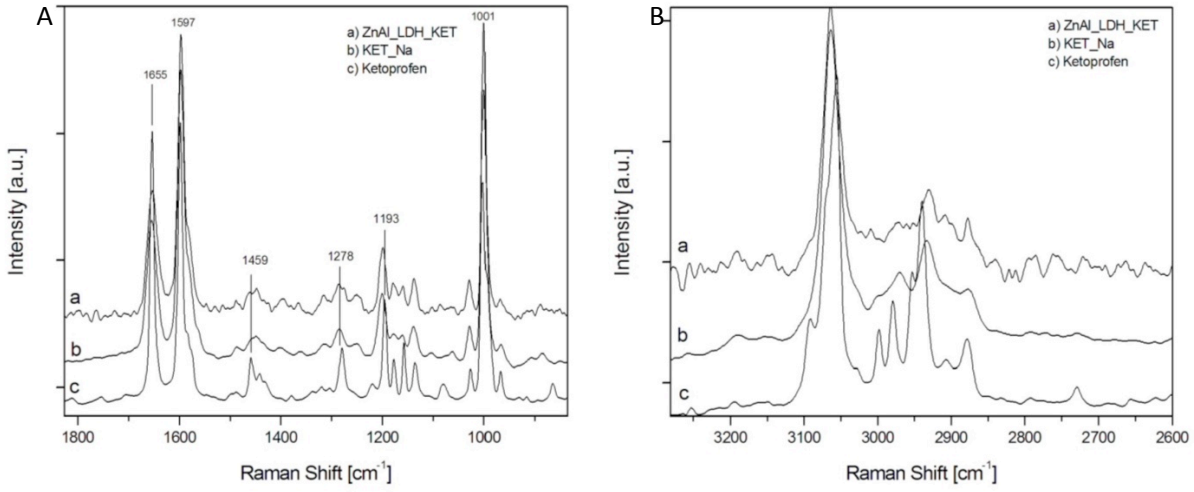

Figure SI5: Raman spectra of Ketoprofen (c), of the sodium salt ketoprofen (b) and of the LDH intercalated compound (a) in the low(A) and high (B) shift region.

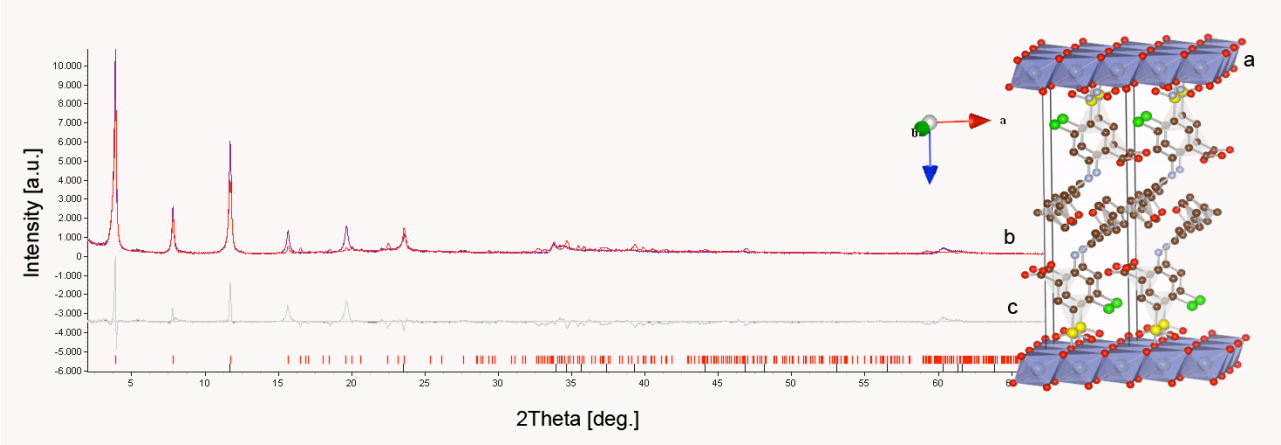

Figure SI6: (a) Approximated crystal structure from structure solution by simulated annealing. The crystal quality hampered the location of a reliable and correct structure, but the packing can be still inferred (R_wp = 26.25). Data are reported in supplementary materials for sake of completeness, as suggested by one of the reviewers. XRPD pattern of Zn/Al_LDH_FURO (b) (in purple the experimental pattern and the calculated one in red); calculated difference curve between experimental pattern and calculated one (c). The ticks on the x axis mark the peak positions for the Zn/Al_LDH_FURO phase (in red) and the Zn/Al_LDH_CO_3 phase (in black) that was added to the fit as its presence in the sample as impurity is unavoidable.

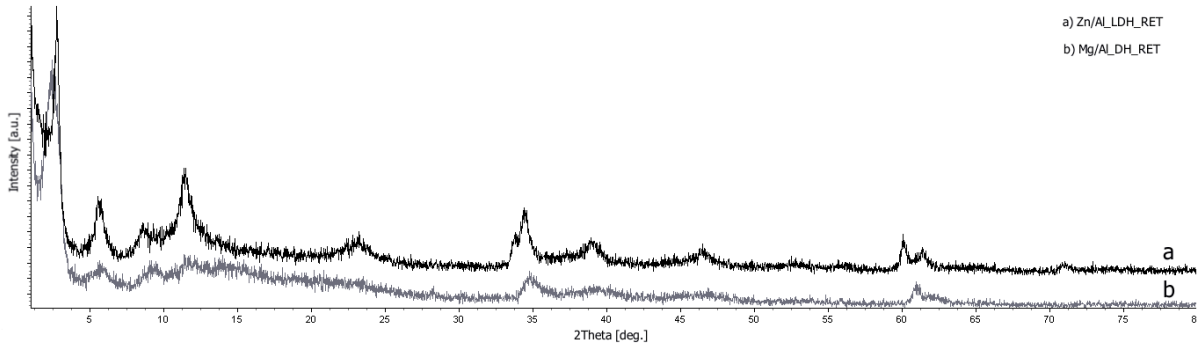

Figure SI7: XRPD powder pattern of Zn/Al_LDH_RET_st (a) and Mg/Al_LDH_RET_st (b)

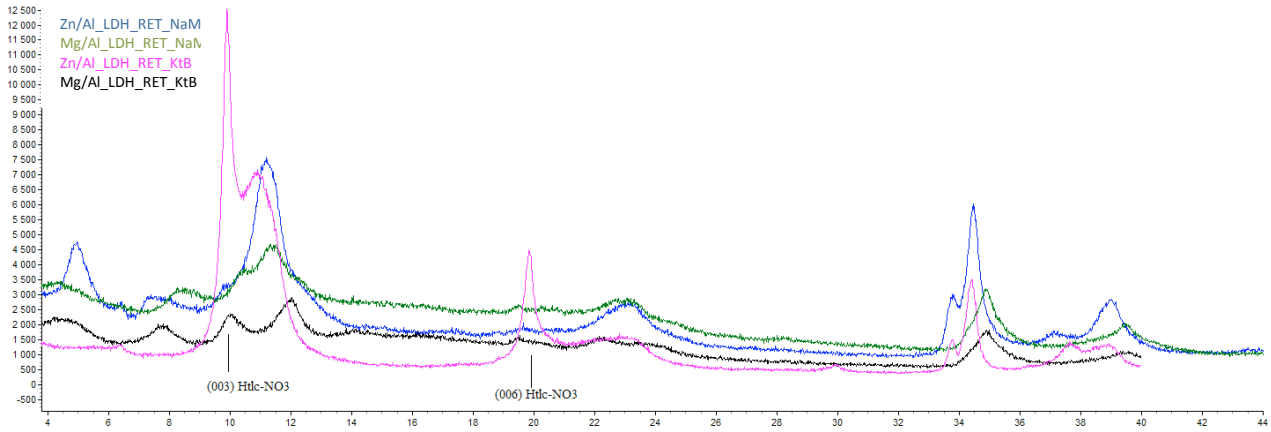

Fig. SI8: XRPD patterns of Zn/Al_LDH_RET_NaM (blue), Mg/Al_LDH_RET_NaM (green), Zn/Al_LDH_RET_KtB (magenta), Mg/Al_LDH _RET_KtB (black).

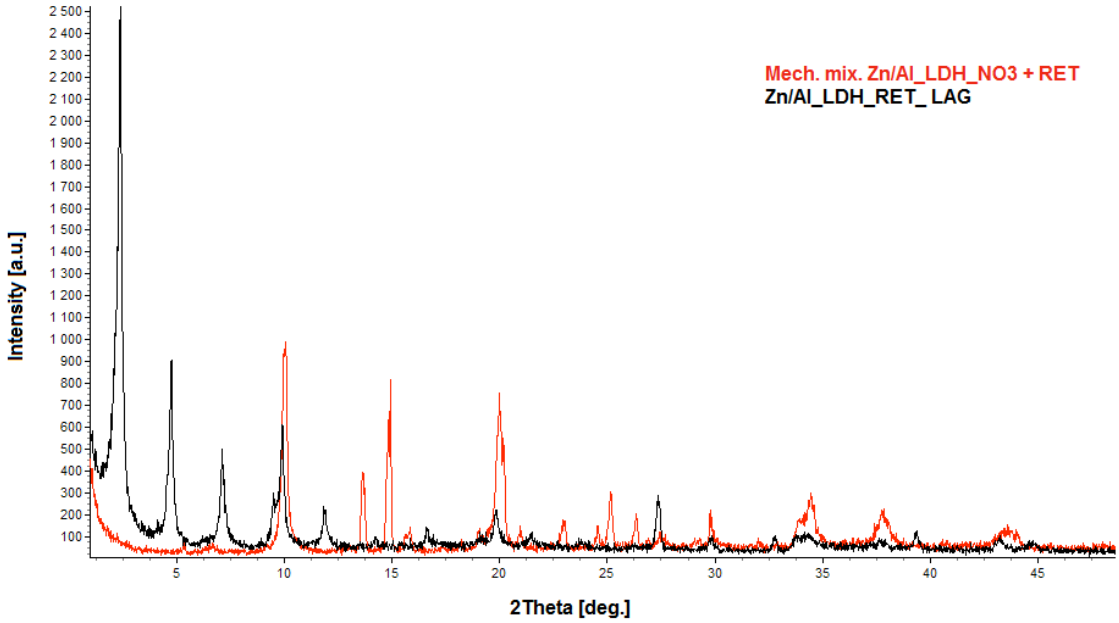

Figure SI9: XRPD pattern of the mechanical mixture of Zn/Al_LDH_NO_3 and retinoic acid (in red) and of the LAG intercalated compound Zn/Al_LDH_RET_LAG (in black)

Table SI1: Crystallographic information of GLICNa and EUSNa single crystal structures

Identification code	EUSNa	GLICNa
Empirical formula	C13 H10 N2 Na O3 S	C15 H20 N3 Na O3 S
Formula weight	297.28	345.39
Temperature	293(2) K	
Wavelength	0.71073 Å	
Crystal system	Orthorombic	Monoclinic
Space group	Pbca	$P2_1/c$
Unit cell dimensions	a = 11.116 Å	a = 15.428 Å
	b = 5.810 Å	b = 9.845 Å
	c = 46.919 Å	c = 12.306 Å
Volume	3030.2 $Å^3$	1759.3 $Å^3$
Z	8	4
Density (calculated)	1.303 Mg/m^3	1.304 Mg/m^3
Absorption coefficient	0.248 mm^{-1}	0.225 mm^{-1}
F(000)	1224	728
Crystal size	0.6 x 0.5 x 0.5 mm^3	0.6 x 0.6 x 0.2 mm^3
Theta range for data collection	4.17 to 30.49°.	4.21 to 30.34°.
Index ranges	-15<=h<=15, -8<=k<=8, -64<=l<=64	-21<=h<=21, -13<=k<=13, -16<=l<=17
Reflections collected	41190	25394
Independent reflections	4401 [R(int) = 0.2358]	4888 [R(int) = 0.0319]
Completeness to theta = 30.49°	95.3 %	92.6 %
Refinement method	Full-matrix least-squares on F^2	
Data / restraints / parameters	4401 / 0 / 208	4888 / 0 / 208
Goodness-of-fit on F^2	1.031	0.904
Final R indices [I>2sigma(I)]	R1 = 0.1190, wR2 = 0.2460	R1 = 0.0576, wR2 = 0.1706
R indices (all data)	R1 = 0.2399, wR2 = 0.2835	R1 = 0.0867, wR2 = 0.2105
Largest diff. peak and hole	0.429 and -0.545 $e.Å^{-3}$	0.569 and -0.407 $e.Å^{-3}$

REFERENCES:

1. L. Perioli, V. Ambrogi, C. Rossi, L. Latterini, M. Nocchetti, and U. Costantino, *J Phys Chem Solids*, 2006, **67**, 1079–1083.

2. V. Ambrogi, G. Fardella, G. Grandolini, M. Nocchetti, and L. Perioli, *J Pharm Sci*, 2003, **92**, 1407–18.

3. V. Ambrogi, L. Perioli, V. Ciarnelli, M. Nocchetti, and C. Rossi, *Eur J Pharm Biopharm*, 2009, **73**, 285–91.

4. V. Ambrogi, G. Fardella, G. Grandolini, L. Perioli, and M. C. Tiralti, *AAPS PharmSciTech*, 2002, **3**, E26.

5. L. Perioli, V. Ambrogi, M. Nocchetti, M. Sisani, and C. Pagano, *Appl .Clay Sci.*, 2011, **53**, 696–703.

6. L. Perioli, V. Ambrogi, B. Bertini, M. Ricci, M. Nocchetti, L. Latterini, and C. Rossi, *Eur J Pharm Biopharm*, 2006, **62**, 185–93.